New Journal of Glass and Ceramics, 2016, 6, 9-17
Published Online April 2016 in SciRes. http://www.scirp.org/journal/njgc
http://dx.doi.org/10.4236/njgc.2016.62002

The Fluorescence of Pr^{3+} in Zinc Lithium Bismuth Borate Glasses with Large Stimulated Emission Cross Section

Beena Bhatia, S. L. Meena

Ceramic Laboratory, Department of Physics, Jai Narain Vyas University, Jodhpur, India
Email: shankardiya7@rediffmail.com

Received 20 December 2015; accepted 2 April 2016; published 5 April 2016

Abstract

Glass sample of Zinc Lithium Bismuth Borate $(25-x)\ Bi_2O_3{:}20Li_2O{:}20ZnO{:}35B_2O_3{:}xPr_6O_{11}$, (where x = 1, 1.5 and 2 mol%) has been prepared by melt-quenching technique. The amorphous nature of the prepared glass samples was confirmed by X-ray diffraction. The absorption spectra of three Pr^{3+} doped zinc lithium bismuth borate glasses have been recorded at room temperature. The observed optical spectra are discussed in terms of energy states and the intensity of the transitions. The various interaction parameters like Slater-Condon, Lande, bonding and Racah parameters have been computed. Judd-Ofelt intensity parameters and laser parameters have also been calculated. The stimulated emission cross section (σ_p) for the transition ($^3P_0 \rightarrow {}^3F_2$) is found to be in the range 3.12 - 10.43 × 10^{-20} cm^2. The σ_p values are comparatively large suggesting the possible utilization of these materials in laser applications.

Keywords

Zinc Lithium Bismuth Borate Glasses, Energy Interaction Parameters, Optical Properties, Judd-Ofelt Analysis

1. Introduction

Rare earth doped solid state materials have become an important class of solids, attracting much attention among researches as is evident from the abundance of studies that can be found in the literature. A substantial amount of work has been done on the lasing characteristics of rare earth doped solid state materials [1] [2].

Glasses are good host for rare earth ions, easy to make and at the same time they can be tailored for specific applications [3]-[5]. Most of the glasses developed for laser action give suitable laser transition in NIR region

How to cite this paper: Bhatia, B. and Meena, S.L. (2016) The Fluorescence of Pr^{3+} in Zinc Lithium Bismuth Borate Glasses with Large Stimulated Emission Cross Section. *New Journal of Glass and Ceramics*, **6**, 9-17.
http://dx.doi.org/10.4236/njgc.2016.62002

whereas Pr^{3+} doped glasses lase in visible region. Praseodymium doped glasses have wide application such as UV-VIS-NIR lasers, up converters, optical fiber amplifier etc. [6]-[8].

Since the spectroscopic properties of rare earth ions are strongly affected by glass composition the host glass composition were tailored with spectroscopic features of Pr^{3+} ion suitable for efficient laser performance.

Some spectral studies have been reported for Pr^{3+} doped borate and phosphate glasses by Weber [9] [10], Riesfeld [11] [12], Lakshman [13] and Tandon *et al*. [14]-[16]. Recently, such studies have been reported on Pr^{3+} doped bismuth borate glasses by our group [17].

In this communication, these studies have been extended by adding higher mol% of Bi_2O_3 in Pr^{3+} doped zinc lithium bismuth borate glasses.

Large stimulated emission cross section is one of the most important parameters required for the design of high peak power solid state lasers. Thus, the variation of σ_p with glass composition (e.g., borate, phosphates, silicates, etc.) has become the subject of intensive study because it is necessary to maximize σ_p to achieve the best performance from an amplifier or laser system [18].

In the present work, the effect of bismuth borate matrix on the fluorescence properties of Pr^{3+} is investigated. The compositional dependence of the stimulated emission cross section of the ($^3P_0 \rightarrow {}^3F_2$) transition of Pr^{3+} is discussed. A comparative study of predicted laser action in borate, phosphate and bismuth borate glasses doped with Pr^{3+} ions have also been discussed. The addition of higher mol% of Bi_2O_3 in borate glasses enhances the value of stimulated emission cross section.

2. Experimental Techniques

Preparation of Glasses

The following Pr^{3+} doped bismuth borate glass samples (25−x) Bi_2O_3:20Li_2O:20ZnO:35B_2O_3:xPr_6O_{11} (where x = 1, 1.5, 2) have been prepared by melt-quenching method. Analytical reagent grade chemical used in the present study consist of Bi_2O_3, Li_2O, ZnO, and B_2O_3 and Pr_6O_{11}. They were thoroughly mixed by using an agate pestle mortar.

Then melted at 1050˚C by an electrical muffle furnace for 2 hours. After complete melting, the melts were quickly poured in to a preheated stainless steel mould and annealed at temperature of 350˚C for 2 h to remove thermal strains and stresses. Every time fine powder of cerium oxide was used for polishing the samples. The glass samples so prepared were of good optical quality and were transparent. The chemical compositions of the glasses with the name of samples are summarized in **Table 1**.

3. XRD Study

Figure 1 represents the XRD pattern of the sample which shows no sharp Bragg's peak, but only a broad diffuse hump around low angle region. This is the clear indication of amorphous nature within the resolution limit of XRD instrument.

The amorphous nature of all samples was confirmed by the absence of Bragg's peak in X-ray diffraction pattern (**Figure 1**).

4. Theory

4.1. Energy Interaction Parameters

The energy E_j can be expressed in terms of interaction parameters-(Slater-Condon) F_k, and ξ_{4f} (Lande) by Taylor

Table 1. Chemical composition of the glasses.

Sample	Glass composition (mol%)
ZnLiBiB (UD)	25Bi_2O_3:20Li_2O:20ZnO:35B_2O_3
ZnLiBiB (PR1)	24Bi_2O_3:20Li_2O:20ZnO:35B_2O_3:1Pr_6O_{11}
ZnLiBiB (PR1.5)	23.5Bi_2O_3:20Li_2O:20ZnO:35B_2O_3:1.5Pr_6O_{11}
ZnLiBiB (PR2)	23Bi_2O_3:20Li_2O:20ZnO:35B_2O_3:2Pr_6O_{11}

ZnLiBiB (UD)—Represents undoped Zinc Lithium Bismuth Borate glass specimens ZnLiBiB (PR)—Represents Pr^{3+} doped Zinc Lithium Bismuth Borate glass specimens.

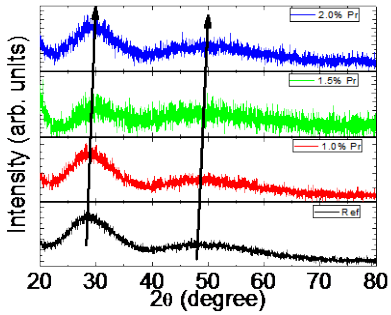

Figure 1. X-ray diffraction pattern of Bi_2O_3:Li_2O:ZnO:B_2O_3:Pr_6O_{11}.

series expansion for a small variation of energies ΔE_j. In the first order approximation, the energy E_j of the j^{th} level is given by [19] [20].

$$E_j\left(F_k,\zeta_{4f}\right)=E_{oj}\left(F^0k,\xi_{4f}\right)+\sum_{k=2,4,6}\frac{\partial E_j}{\partial F_k}\Delta F_k+\frac{\partial E_j}{\partial \xi_{4f}}\Delta\xi_{4f},\ k=2,4,6 \tag{1}$$

where, E_{oj} is the zero order energy of j^{th} level and ΔF_k and $\Delta\xi_{4f}$ are the small changes in the corresponding parameters and these values have been calculated by partial regression method.

The value of F_k and ξ_{4f} are then evaluated using equations.

$$F_k=F_k^0+\Delta F_k^0 \tag{2}$$

$$\xi_{4f}=\xi_{4f}^0+\xi_{4f} \tag{3}$$

where, F_k^0 and ξ_{4f}^0 are zero order values of the parameters F_k and ξ_{4f}, respectively.

The Racah parameters E^k (k = 1, 2, 3) can be expressed as linear combination of F_k (k = 2, 4, 6) given by

$$E^1=\left(70F_2+231F_4+2002F_6\right)/9 \tag{4}$$

$$E^2=\left(F_2-3F_4+7F_6\right)/9 \tag{5}$$

$$E^3=\left(5F_2+6F_4-91F_6\right)/3 \tag{6}$$

4.2. Oscillator Strength

The intensity of spectral lines are expressed in terms of oscillator strengths using the relation [21].

$$f_{\text{expt}}=4.318\times10^{-9}\int\varepsilon(\nu)\,\mathrm{d}\nu \tag{7}$$

where, $\varepsilon(v)$ is molar absorption coefficient at a given energy v (cm^{-1}), to be evaluated from Beer-Lambert law.

Under Gaussian Approximation, using Beer-Lambert law, the observed oscillator strengths of the absorption bands have been experimentally calculated, using the modified relation [22].

$$P_m=4.6\times10^{-9}\times\frac{1}{cl}\log\frac{I_0}{I}\times\Delta\upsilon_{1/2} \tag{8}$$

where c is the molar concentration of the absorbing ion per unit volume, I is the optical path length, $\log I_0/I$ is absorbtivity or optical density and $\Delta\upsilon_{1/2}$ is half band width.

4.3. Judd-Ofelt Intensity Parameters

According to Judd [23] and Ofelt [24] theory, independently derived expression for the oscillator strength of the induced forced electric dipole transitions between an initial J manifold $\left|4f^N(S,L)J\right\rangle$ level and the terminal J' manifold $\left|4f^N(S',L')J'\right\rangle$ is given by:

$$\frac{8\Pi^2 mc\bar{\upsilon}}{3h(2J+1)}\frac{1}{n}\left[\frac{\left(n^2+2\right)^2}{9}\right]\times S\left(J,J'\right) \tag{9}$$

where, the line strength $S\left(J,J'\right)$ is given by the equation

$$S\left(J,J'\right)=e^2\sum_{\lambda=2,4,6}\Omega_\lambda <4f^N\left(S,\ L\right)J\left\|U^{(\lambda)}\right\|4f^N\left(S',L'\right)J'>2,\ \lambda=2,4,6 \tag{10}$$

In the above equation m is the mass of an electron, c is the velocity of light, v is the wave number of the transition, h is Planck's constant, n is the refractive index, J and J' are the total angular momentum of the initial and final level respectively, Ω_λ (λ = 2, 4 and 6) are known as Judd-Ofelt intensity parameters which contain the effect of the odd-symmetry crystal field terms, radial integrals and energy denominators. $\left\|U^{(\lambda)}\right\|^2$ are the matrix elements of the doubly reduced unit tensor operator calculated in intermediate coupling approximation. Ω_λ parameter can be obtained from least square fitting method [25]. The matrix element $\left\|U^{(\lambda)}\right\|^2$ that are insensitive to the environment of rare earth ions were taken from the literature [26].

4.4. Radiative Properties

The Ω_λ parameters obtained using the absorption spectral results have been used to predict radiative properties such as spontaneous emission probability (A) and radiative life time (τ_R), and laser parameters like fluorescence branching ratio (β_R) and stimulated emission cross section (σ_p).

The spontaneous emission probability from initial manifold $\left|4f^N\left(S',L'\right)J'\right\rangle$ to a final manifold $\left|4f^N\left(S,L\right)J\right\rangle$ is given by:

$$A\left[\left(S',L'\right)J';\left(S,L\right)J\right]=\frac{64\pi^2\nu^3}{3h\left(2J'+1\right)}\frac{n\left(n^2+2\right)^2}{9}\times S\left(J',\bar{J}\right) \tag{11}$$

where, $S\left(J',J\right)=e^2\left[\Omega_2\left\|U^{(2)}\right\|+\Omega_4\left\|U^{(4)}\right\|^2+\Omega_6\left\|U^{(6)}\right\|^2\right]$

The fluorescence branching ratio for the transitions originating from a specific initial manifold $\left|4f^N\left(S',L'\right)J'\right\rangle$ to a final many fold $\left|4f^N\left(S,L\right)J\right\rangle$ is given by

$$\beta\left[\left(S',L'\right)J';\left(S,L\right)J\right]=\frac{A\left[\left(S'L\right)\right]}{\sum_{SLJ}A\left[\left(S'L'\right)J'\left(\bar{S}L\right)\right]} \tag{12}$$

where, the sum is over all terminal manifolds.

The radiative life time is given by

$$\tau_{rad}=\sum_{SLJ}A\left[\left(S',L'\right)J';\left(\bar{S},L\right)\right]=A_{Total}^{-1} \tag{13}$$

where, the sum is over all possible terminal manifolds. The stimulated emission cross -section for a transition from an initial manifold $\left|4f^N\left(S',L'\right)J'\right\rangle$ to a final manifold $\left|4f^N\left(S,L\right)J\right\rangle$ is expressed as

$$\sigma_p\left(\lambda_p\right)=\left[\frac{\lambda_p^4}{8\pi cn^2\Delta\lambda_{eff}}\right]\times A\left[\left(S',L'\right)J';\left(\bar{S},\bar{L}\right)\bar{J}\right] \tag{14}$$

where, λ_p the peak fluorescence wavelength of the emission band and $\Delta\lambda_{eff}$ is the effective fluorescence line width.

4.5. Nephelauxetic Ratio (β') and Bonding Parameter ($b^{1/2}$)

The nature of the R-O bond is known by the Nephelauxetic Ratio $\left(\beta'\right)$ and Bonding Parameter ($b^{1/2}$), which

are computed by using following formulae [27]. The Nephelauxetic Ratio is given by

$$\beta' = \frac{\nu_g}{\nu_a} \tag{15}$$

where, ν_a and ν_g refer to the energies of the corresponding transition in the glass and free ion, respectively. The values of bonding parameter $b^{1/2}$ are given by

$$b^{1/2} = \frac{1-\bar{\beta}}{\bar{\beta}} \tag{16}$$

where $\bar{\beta}$ is the average value of β'.

5. Results and Discussion

5.1. Optical Properties

Absorption Spectrum

The absorption spectra of these glasses were recorded between wavelengths range 400 - 900 nm with a Spctro Scan 80D/80DV Spectrophotometer and 900 - 2250 nm with a Perkin-Elmer Lambda 750 UV/VIS/NIR Spectrophotometer at room temperature.

The absorption spectra of Pr^{3+} doped ZnLiBiB glass specimens have been represented in **Figure 2** in terms of relative absorption (I/I_0) versus wavelength (nm), where I and I_0 are intensities of the radiation transmitted through doped specimens and undoped specimens of equal thickness. Eight absorption bands UV-VIS and NIR region have been observed from the ground state $^3H_4$to excited states $^3P_2$, $^3P_1$, $^3P_0$, $^1D_2$, $^1G_4$, $^3F_4$, $^3F_3$ and $^3F_2$ for Pr^{3+} doped ZnLiBiB glasses.

The optical absorption bands around the $^3P_2$ (446 nm), $^3P_1$ (469 nm), $^3P_0$ (485 nm), $^1D_2$ (592 nm), $^1G_4$ (1010 nm), $^3F_4$ (1442 nm), $^3F_3$ (1527 nm) and $^3F_2$ (1936 nm), are assigned from the ground state, $^3H_4$, Assignment have been made by published article [28]. From the absorption spectra, experimental oscillator strengths have been calculated for all the absorption bands.

The experimental and calculated oscillator strengths for Pr^{3+} ions in zinc lithium bismuth borate glasses are given in **Table 2**. Racah parameters (E^k) have been deduced from F_k parameters [29] (**Table 3**). The ratio of Racah parameters E^1/E^3 and E^2/E^3 are about 10 and 0.05 respectively. Which are almost equal to the hydrogenic ratio [30]. This implies that Pr^{3+} ions at different doping concentrations are subjected.

Further Judd-Ofelt intensity parameters Ω_λ (λ = 2, 4 and 6) were calculated by using the fitting approximation of the experimental oscillator strengths to the calculated oscillator strengths with respect to their electric dipole contributions. In the present case the three Ω_λ parameters follow the trend $\Omega_2 < \Omega_4 < \Omega_6$. The spectroscopic quality factor (Ω_4/Ω_6) related with the rigidity of the glass system has been found to lie between 0.4 and 0.7 in the

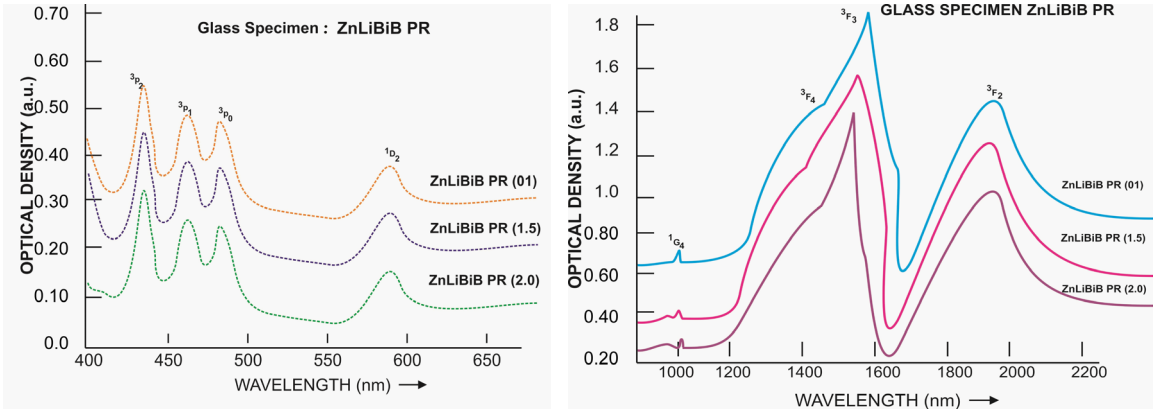

(a) (b)

Figure 2. (a) Absorption spectrum of ZnLiBiB glasses doped with Pr^{3+} inUV-VIS region; (b) Absorption spectrum of ZnLiBiB glasses doped with Pr^{3+} in NIR region.

Table 2. Measured and calculated oscillator strength ($P_m \times 10^{+6}$) of Pr^{3+} ions in ZnLiBiB glasses.

Energy level from $^3H_4$	Glass ZnLiBiB (PR01)		Glass ZnLiBiB (PR1.5)		Glass ZnLiBiB (PR02)	
	$P_{exp.}$	$P_{cal.}$	$P_{exp.}$	$P_{cal.}$	$P_{exp.}$	$P_{cal.}$
$^3F_2$	4.121	3.556	3.23	2.792	2.12	1.838
$^3F_3$	7.82	6.916	6.126	5.355	5.125	4.440
$^3F_4$	4.435	4.315	3.226	3.317	2.112	2.682
$^1G_4$	0.482	0.362	0.360	0.279	0.240	0.229
$^1D_2$	3.241	1.234	2.12	0.952	1.116	0.783
$^3P_0$	4.321	1.869	3.226	1.510	2.154	1.512
$^3P_1$	4.128	3.183	3.125	2.541	2.106	2.406
$^3P_2$	11.12	4.116	10.107	3.175	9.816	2.623
r.m.s. deviation	±2.776		±2.586		±2.579	

Table 3. Computed values of Slater-Condon, Lande, Racah, nephelauexetic ratio and bonding parameter for Pr^{3+} doped ZnLiBiB glass specimens.

Parameter	Free ion	ZnLiBiB PR01	ZnLiBiB PR1.5	ZnLiBiB PR02
F_2 (cm^{-1})	322.09	299.62	299.21	298.83
F_4 (cm^{-1})	44.46	44.36	44.35	44.28
F_6 (cm^{-1})	4.867	4.427	4.407	4.397
ξ_{4f} (cm^{-1})	741.00	856.74	856.80	858.36
E^1 (cm^{-1})	4728.92	4453.71	4445.82	4438.84
E^2 (cm^{-1})	24.75	21.95	21.89	21.86
E^3 (cm^{-1})	478.10	453.80	453.70	453.23
F_4/F_2	0.13805	0.14805	0.14822	0.14818
F_6/F_2	0.01511	0.01478	0.01473	0.01471
E^1/E^3	9.8911	9.8143	9.7990	9.7938
E^2/E^3	0.0518	0.0484	0.0483	0.0482
β'		0.9302	0.9290	0.9278
$b^{1/2}$		0.1868	0.1884	0.1900

present glasses. The values of Judd-Ofelt intensity parameters are given in **Table 4**.

A comparison of calculated σ values for bismuth borate glasses with those reported [31] for borate, silicate, fluoroberyllate, phosphate and tellurite glasses (**Figure 3**) shows that bismuth borate glasses are best and tellurite glasses the next best. However, tellurite glasses have low transmission in the desired region (NIR) due to high value of refractive index.

Computed values of Slater-Condon, Lande, Racah, nephelauexetic ratio and bonding parameter for Pr^{3+} doped ZnLiBiB glass specimens are given in **Table 3**.

5.2. Fluorescence Spectrum

The fluorescence spectrum of Pr^{3+}doped in zinc lithium bismuth borate glass is shown in **Figure 4**. There are four broad bands ($^3P_0 \rightarrow {}^3H_4$), ($^3P_0 \rightarrow {}^3H_5$), ($^3P_0 \rightarrow {}^3H_6$) and ($^3P_0 \rightarrow {}^3F_2$), respectively for glass specimens. Out of four emission transition observed from$^3P_0$level, only three ($^3P_0 \rightarrow {}^3H_4$, $^3H_6$ and $^3F_2$) are included in the fit. The transition $^3P_0 \rightarrow {}^3H_5$ is excluded since the matrix elements for this transition are zero and the β is too weak to measure.

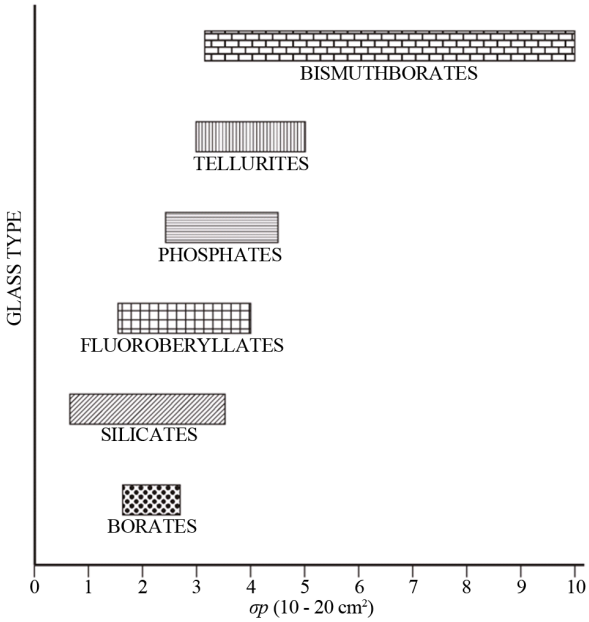

Figure 3. Range of stimulated emission cross-section for different Pr^{3+} doped glasses.

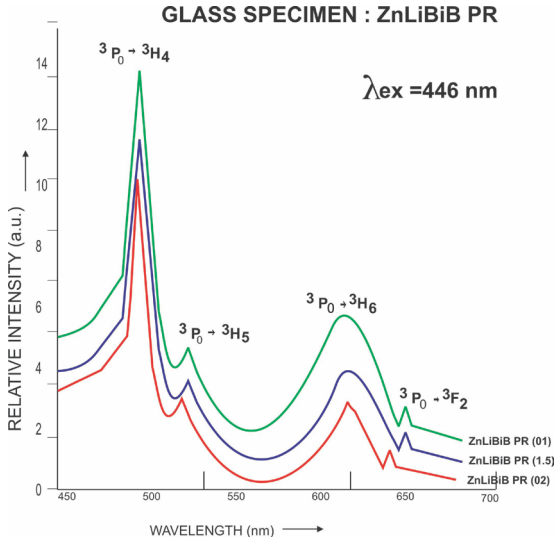

Figure 4. Fluorescence spectrum of ZnLiBiB glasses doped with Pr^{3+}.

Table 4. Judd-Ofelt intensity parameters for Pr^{3+} doped ZnLiBiB glass specimens.

Glass Specimen	Ω_2 (pm^2)	Ω_4 (pm^2)	Ω_6 (pm^2)	Ω_4/Ω_6
ZnLiBiB (PR01)	1.90	2.41	5.58	0.432
ZnLiBiB (PR1.5)	1.48	1.94	4.27	0.454
ZnLiBiB (PR02)	0.549	1.95	3.47	0.763

The value of stimulated emission cross-section (σ_p) is found to be maximum for the transition ($^3P_0 \rightarrow {}^3F_2$) for glass ZnLiBiB PR 01, suggesting that glass ZnLiBiB PR01 is better compared to the other two glass systems (ZnLiBiB PR1.5 and ZnLiBiB PR02). The wavelengths of these bands along with their assignments are given in **Table 5**.

Table 5. Emission peak wave lengths (λ_p), radiative transition probability (A_{rad}), branching ratio (β_R), stimulated emission cross-section (σ_p), andradiative life time (τ) for various transitions in Pr^{3+} doped ZnLiBiB glasses.

Transition	ZnLiBiB PR 01					ZnLiBiB PR 1.5				ZnLiBiB PR 02			
	λ_p (nm)	A_{rad} (s^{-1})	β_R	σ_p (10^{-20} cm^2)	τ (μs)	A_{rad} (s^{-1})	β_R	σ_p (10^{-20} cm^2)	τ (μs)	A_{rad} (s^{-1})	β_R	σ_p (10^{-20} cm^2)	τ (μs)
$^3P_0 \rightarrow {}^3H_4$	485	16584.29	0.4755	2.385	60.302	13483.39	0.4880	1.871	74.079	13499.6	0.6251	1.746	74.076
$^3P_0 \rightarrow {}^3H_5$	528	-	-	-	-	-	-	-	-	-	-	-	-
$^3P_0 \rightarrow {}^3H_6$	610	8575.56	0.2459	3.585	116.610	6566.73	0.2377	2.638	189.204	5285.30	0.2447	2.042	189.20
$^3P_0 \rightarrow {}^3F_2$	643	9715.70	0.2786	10.434	102.93	7578.47	0.2743	8.29	355.736	2811.07	0.1302	3.12	355.74

6. Conclusion

In the present study, the glass samples of composition $(25-x)$ Bi_2O_3:$20Li_2O$:$20ZnO$:$35B_2O_3$:xPr_6O_{11} (where x = 1, 1.5, 2 mol%) have been prepared by melt-quenching method. The stimulated emission cross section (σ_p) and branching ratio (β_R) values are calculated for present glasses. It could be observed that glass ZnLiBiB (PR01) possessed better values when compared to the other two glass systems. The large stimulated emission cross section in bismuth borate glasses suggests the possibility of utilizing these systems as laser materials.

Acknowledgements

Our sincere thanks to Prof. R.J. Sengwa, Head Department of physics for providing chemicals. (Rare Earths) I.I.T. Jodhpur, Defence lab, Jodhpur, are hereby acknowledged for providing facilities for sample preparation, spectral and X-ray measurements. The authors wish to express heartiest gratitude to Prof. S.P. Tandon, Retired Prof. of physics, J.N.V. University, Jodhpur, Dr. M.P. Bhutra Retired Associate Professor of physics J.N.V. University, Jodhpur for valuable suggestions.

References

[1] Sharma, Y.K., Tandon, S.P. and Surana, S.S.L. (2000) Laser Action in Praseodymium Doped Zinc Chloride Borophosphate Glasses. *Journal of Materials Science and Engineering B*, **77**, 167-171. http://dx.doi.org/10.1016/S0921-5107(00)00471-2

[2] Tandon, S.P., Sharma, Y.K., Bishnoi, N.B. and Tandon, K. (1997) Optical Studies on Rare Earth Lasing Materials. *Journal of Defence Science*, **47**, 225-238. http://dx.doi.org/10.14429/dsj.47.4004

[3] Zhou, S., Jiang, N., Zhu, B., Yang, H., Ye, S., Laksminarayana, G., Hao, J. and Qiu, J. (2008) Multifunctional Bismuth-Doped Nanoporous Silica Glass: From Blue-Green, Orange, Red and White Light Sources to Ultra-Broadband Infrared Amplifiers. *Advanced Functional Materials*, **18**, 1407-1413. http://dx.doi.org/10.1002/adfm.200701290

[4] Meng, X.G., Qiu, J.R., Peng, M.Y., Chen, D.P., Zhao, Q.Z., Jiang, X.W. and Zhu, C.S. (2005) Near Infrared Broadband Emission of Bismuth-Doped Aluminophosphate Glass. *Optics Express*, **13**, 1628-1634. http://dx.doi.org/10.1364/OPEX.13.001628

[5] Wang, Y., Dai, S., Chen, F., Xu, T. and Nie, Q. (2009) Physical Properties and Optical Band Gap of New Tellurite Glasses within the TeO_2-Nb_2O_5-Bi_2O_3 System. *Materials Chemistry and Physics*, **113**, 407-411. http://dx.doi.org/10.1016/j.matchemphys.2008.07.117

[6] Lu, M.H. and Sturm, J.C. (2002) Optimization of External Coupling and Light Emission in Organiclight-Emitting Devices: Modeling and Experiment. *Journal of Applied Physics*, **91**. http://dx.doi.org/10.1063/1.1425448

[7] Vijay Prakash, G. (2000) Absorption Spectral Studies of Rare Earth Ions (Pr^{3+}, Nd^{3+}, Sm^{3+}, Dy^{3+}, Ho^{3+} and Er^{3+}) Doped in NASICON Type Phosphate Glass, $Na_4AlZnP_3O_{12}$. *Journal of Materials Letters*, **46**, 15-20.

[8] Rai, V.K., de S. Menezes, L. and de Araújo, C.B. (2007) Spectroscopy, Energy Transfer and Frequency Upconversion in Tm^{3+}-Doped TeO_2-PbO Glass. *Journal of Applied Physics*, **102**, Article ID: 043505. http://dx.doi.org/10.1063/1.2769788

[9] Weber, M.J. (1982) Hand Book of Laser Science and Technology. Vol. 1, CRC, Boca Raton.

[10] Weber, M.J., Ziebier, D.C. and Angell, C.A. (1982) Tailoring Stimulated Emission Cross Section of Nd^{3+} Laser Glass: Observation of Large Cross Section for $BiCl_3$ Glasses. *Journal of Applied Physics*, **53**, 4344. http://dx.doi.org/10.1063/1.331214

[11] Reisfeld, R. (1985) Luminescence and Predication of Transition Probabilities for Solar Energy and Lasers. *Journal of the Less Common Metals*, **112**, 9-18.

[12] Hormadaly, J. and Reisfeld, R. (1979) Intensity Parameters and Laser Analysis of Pr^{3+} and Dy^{3+} in Oxide Glasses. *Journal of Non-Crystalline Solids*, **30**, 337-348.

[13] Lakashman, S.V.J. and Kumar, A.S. (1986) Evaluation of Spectroscopic Parameters for Pr^{3+} Ion in Potassium Zinc Sulphate Glass. *Journal of Non-Crystalline Solids*, **85**, 162-169. http://dx.doi.org/10.1016/0022-3093(86)90088-8

[14] Sharma, Y.K., Mathur, S.C., Dube, D.C. and Tandon, S.P. (1996) Electrical and Optical Band Gap Studies in Neodymium Borophosphate Glasses. *Journal of Materials Science*, **15**, 1054-1056. http://dx.doi.org/10.1007/bf00274904

[15] Sharma, Y.K., Bishnoi, N.B., Surana, S.S.L. and Tandon, S.P. (1992) Spectral Studies of Pr^{3+}, Sm^{3+} and Ho^{3+} Ions in Sodium Barium Borate Glass. *Journal of Pure and Applied Physics*, **4**, 200-211.

[16] Tandon, S.P., Bishnoi, N.B., Sharma, Y.K. and Surana, S.S.L. (1995) Dependence of Fluorescence Spectra of Pr^{3+} Doped Chlorophosphate Glasses on Doping Concentration. *Journal of Physics*, **11**, 93-97.

[17] Bhatia, B., Parihar, V., Singh, S. and Verma, A.S. (2013) Spectroscopic Properties of P^{r3+} in Lithium Bismuth Borate Glasses. *American Journal of Condensed Matter Physics*, **3**, 80-88.

[18] Saisudha, M.B., Koteswara, K.S.R., Bhat, H.L. and Ramakrishna, J. (1996) The Fluorescence of Nd^{3+} in Lead Borate and Bismuth Borate Glasses with Large Stimulated Emission Cross Section. *Journal of Applied Physics*, **80**, 4845. http://dx.doi.org/10.1063/1.363520

[19] Wong, E.J. (1963) Configuration Interaction of the Pr^{3+} Ion. *The Journal of Chemical Physics*, **38**, 976-978. http://dx.doi.org/10.1063/1.1733794

[20] Wong, E.J. (1961) Tayler Series Expansion of the Intermediate Coupling Energy Levels of Nd^{3+} and Er^{3+}. *The Journal of Chemical Physics*, **35**, 544-546. http://dx.doi.org/10.1063/1.1731965

[21] Gorller-Walrand, C. and Binnemans, K. (1988) Spectral Intensities of f-f Transition. In: Gshneidner Jr., K.A. and Eyring, L., Eds., *Handbook on the Physics and Chemistry of Rare Earths*, Vol. 25, Chap. 167, North-Holland, Amsterdam, 101-264.

[22] Sharma, Y.K., Surana, S.S.L. and Singh, R.K. (2009) Spectroscopic Investigations and Luminescence Spectra of Sm^{3+} Doped Soda Lime Silicate Glasses. *Journal of Rare Earths*, **27**, 773-780. http://dx.doi.org/10.1016/S1002-0721(08)60333-6

[23] Judd, B.R. (1962) Optical Absorption Intensities of Rare Earth Ions. *Physical Review*, **127**, 750-761. http://dx.doi.org/10.1103/PhysRev.127.750

[24] Ofelt, G.S. (1962) Intensities of Crystal Spectra of Rare Earth Ions. *The Journal of Chemical Physics*, **37**, 511. http://dx.doi.org/10.1063/1.1701366

[25] Goublen, C.H. (1964) Methods of Statistical Analysis. Asian Publishing House, Bombay, Chap. 8, 138.

[26] Babu, P. and Jayasankar, C.K. (2001) Spectroscopy of Pr^{3+} Ions in Lithium Borate and Lithium Fluoroborate Glasses. *Physica B*: *Condensed Matter*, **301**, 326-340. http://dx.doi.org/10.1016/S0921-4526(01)00239-3

[27] Sinha, S.P. (1996) Complexes of the Rare Earths. Pergamon Press, Oxford.

[28] Pal, I., Agarwal, A., Sanghi, S. and Aggarwal, M.P. (2011) Structural, Absorption and Fluorescence Spectral Analysis of Pr^{3+} Ions Doped Zinc Bismuth Borate Glasses. *Journal of Alloys and Compounds*, **509**, 7625-7631. http://dx.doi.org/10.1016/j.jallcom.2011.04.114

[29] Sharma, Y.K. (1991) Spectral and Electoral Properties of Lanthanide Ions in Different Environment. PhD Thesis, University of Jodhpur, Jodhpur.

[30] Dieke, G.H. (1968) Spectra and Energy Levels of Rare Earth Ions in Crystals. InterScience, Johan Wiley and Sons, New York.

[31] Weber, M.J. (1983) Recent Development in Laser Glasses. *Proceedings of the International Conference on Lasers*, New Orleans, 55-63.